ACTA ABP BIOCHIMICA POLONICA

Vol. 70, No 4/2023
919–925
https://doi.org/10.18388/abp.2020_6819

Regular paper

Hepatic Mcpip1 regulates adaptation to food restriction in mice

Olga Mucha[1], Bozena Skupien-Rabian[2&], Alicja Slota[1#&], Katarzyna Trzos[1#], Natalia Pydyn[1], Bartosz Podlewski[1], Jolanta Jura[1] and Jerzy Kotlinowski[1]

[1]Jagiellonian University, Faculty of Biochemistry, Biophysics and Biotechnology, Department of General Biochemistry, Kraków, Poland; [2]Jagiellonian University, Malopolska Centre of Biotechnology, Proteomics and Mass Spectrometry Core Facility, Kraków, Poland

Monocyte-chemoattractant protein-induced protein 1 (MCPIP1, or Regnase-1) is an endoribonuclease that degrades translationally active mRNA molecules. MCPIP1 is mostly known for its anti-inflammatory actions, but it is also an important regulator of adipogenesis and lipid metabolism. Its overexpression impairs adipogenesis by reducing mRNA levels of C/EBPβ and PPARγ, key transcription factors regulating this process. Although adipocytes overexpressing MCPIP1 are characterised by impaired glucose uptake, the function of MCPIP1 in hepatocyte metabolism remains unknown. In this study, conditional deletion of *Zc3h12a* in murine liver epithelial cells was used to characterise the role of Mcpip1 in adaptation to 24-hour food restriction. We found that Mcpip1 deficiency in liver epithelial cells (Mcpip1$^{fl/fl}$Alb^{Cre} mice) resulted in higher blood glucose levels in response to fasting in comparison to Mcpip1$^{fl/fl}$ counterparts. Hepatic proteome analysis showed 26 down-regulated and 117 up-regulated proteins in Mcpip1$^{fl/fl}$Alb^{Cre} animals that were involved in cellular adhesion, extracellular matrix and metabolic processes. In conclusion, our studies provide new insight into the hepatic function of Mcpip1 and its involvement in metabolic control.

Keywords: MCPIP1, liver, fasting, feeding, food restriction

Received: 27 April, 2023; revised: 28 July, 2023; accepted: 21 September, 2023; available on-line: 06 November, 2023

e-mail: j.kotlinowski@uj.edu.pl
#current affiliation: Jagiellonian University, Doctoral School of Exact and Natural Sciences, Kraków, Poland
&equal contribution as a second author

Acknowledgements of Financial Support: This work was supported by a research grant from the National Science Centre, Poland, No. 2017/27/B/NZ5/01440 to JK.

Abbreviations: DAVID, Database for Annotation, Visualization and Integrated Discovery; FDR, false discovery rate; HSCs, hepatic stellate cells; MCPIP1, Monocyte-chemoattractant protein-induced protein 1; NAFLD, Non-alcoholic fatty liver disease

INTRODUCTION

Both humans and animals adjust their metabolism to an excess or deficiency of food and the liver plays a central role in these processes. During the shift from a feeding to a fasting state, hepatic production of glucose and ketone bodies increases, with concomitant glycogen depletion and triacylglycerol accumulation (Goldstein & Hager, 2015). In contrast, a meal containing carbohydrates stimulates hepatic glucose uptake and glycolysis and repletes glycogen stores. Fatty acid synthesis is induced, while β-oxidation and ketogenesis are inhibited (Moore *et al.*, 2012). As a result, high-energy stores are replenished both in hepatocytes and adipocytes, maintaining metabolic homeostasis during periods of feeding and fasting (Geisler *et al.*, 2016).

Monocyte-chemoattractant protein-induced protein 1 (MCPIP1), encoded by the *ZC3H12A* gene, is mostly known for its anti-inflammatory properties. It is an endoribonuclease that degrades mRNA, pre-miRNA, and viral RNA molecules. The broad spectrum of MCPIP1 targets includes IL-1β (Mizgalska *et al.*, 2009), IL-6 (Matsushita *et al.*, 2009) and IL-2 (Li *et al.*, 2012). MCPIP1 was also shown to regulate glucose and lipid metabolism and its hepatic levels are reduced in humans suffering from Non-alcoholic fatty liver disease (NAFLD) (Pydyn *et al.*, 2023). MCPIP1 inhibits adipogenesis *in vitro* by reducing the levels of key transcription factors, including C/EBPβ (Lipert *et al.*, 2017). Additionally, adipocytes that overexpress the MCPIP1 protein are characterised by a lower level of the insulin receptor Glut4 and impaired glucose uptake (Losko *et al.*, 2020).

In this study, we aimed to analyse the role of hepatic Mcpip1 in murine adaptation to fasting. We performed mass spectrometry analysis of whole-liver lysates from Mcpip1$^{fl/fl}$ and Mcpip1$^{fl/fl}$Alb^{Cre} mice that were fasted for 24 h, followed by functional annotation and enrichment analysis of differentially expressed proteins. We demonstrated that Mcpip1 is involved in the regulation of metabolic pathways, including glyoxylate and dicarboxylate metabolism or the pentose phosphate pathway. Our studies provide new insight into the hepatic function of Mcpip1 and its involvement in metabolic control.

MATERIAL AND METHODS

Animals and genotyping

The study used 10-week-old female control Zc3h12a$^{lox/lox}$ mice (designed as Mcpip1$^{fl/fl}$) and Mcpip1 liver epithelial cell-specific knockout mice (designed as Mcpip1$^{fl/fl}$Alb^{Cre}). Deletion of Mcpip1 protein in Mcpip1$^{fl/fl}$Alb^{Cre} mice was present in liver epithelial cells (hepatocytes and cholangiocytes). Its level in whole liver tissue was only partially reduced (Kotlinowski *et al.*, 2021). The animals were genotyped as previously described (Kotlinowski *et al.*, 2021). In brief, DNA was extracted from tail tissue using a KAPA Mouse Genotyping Kit (KAPA Biosystems) according to the manufacturer's instructions. Genotyping for loxP insertion was performed by PCR using the following primers: GCCTTCCTGATCCTATTGGAG (wild-type), GAGATGGCGCAGCGCAATTAAT (knockout), and GCCTCTTGTCACTCCCTCCTCC (common). Genotyping for AlbCre tg/+ was conducted with the following primers: TGCAAACATCACATGCACAC (wild-type), GAAGCAGAAGCTTAGGAA-

GATGG (mutant), and TTGGCCCCTTACCATAACTG (common). The animals were housed under SPF conditions in ventilated cages in a temperature-controlled environment with a 14-h light/10-h dark cycle. The mice were randomly divided into 'fed' and 'fasted' groups at 10 weeks of age. Mice from the fed group received food and water *ad libitum*, whereas the animals enrolled in the 'fasted' group were placed into cages containing only water for 24 hours. On the following day, all animals were sacrificed, and blood and liver were collected. All animal procedures were conducted in accordance with the Guide for the Care and Use of Laboratory Animals (Directive 2010/63/EU of the European Parliament) and carried out under a licence from the 2nd Local Institutional Animal Care and Use Committee in Krakow (study no. 272/2017).

Blood analysis

All blood tests were measured by an automated analyser (Arkray) according to the manufacturer's instructions.

Protein isolation and western blot

Liver samples were lysed using RIPA buffer (25 mM Tris-HCl; pH 7.6; 150 mM NaCl, 1% sodium deoxycholate and 0.1% SDS) with Complete Protease Inhibitor Cocktail (Roche) and PhosSTOP Phosphatase Inhibitor Cocktail (Roche). A bicinchoninic acid assay was used to assess protein concentration, and 25 μg of proteins were separated on a 10% SDS/PAGE polyacrylamide gel. After wet transfer to PVDF membranes (Millipore), the membranes were blocked in 5% skim milk and then incubated overnight with primary antibodies at 4°C. On the following day, the membranes were washed and incubated with a secondary antibody for 1 h at room temperature. Chemiluminescence was detected after 5 min of incubation with ECL™ Select Western Blotting Detection Reagent (GE Healthcare) in a ChemiDoc chemiluminescence detector (Bio-Rad). The following antibodies were used: rabbit anti-MCPIP1 (1:2000; GeneTex), rabbit anti-PPARγ (1:1000; Cell Signaling), mouse anti-β-actin (1:4000; Sigma), peroxidase-conjugated anti-rabbit (1:30 000; Cell Signaling) and peroxidase-conjugated anti-mouse (1:20 000; BD).

LC-MS/MS analysis and data processing

Liver fragments were homogenised in lysis buffer (7M urea, 2M thiourea, 4% CHAPS and 30 mM Tris; pH 7.5) using a CTFE/stainless steel pestle. Then, dithiothreitol was added at a concentration of 50 mM and the tissue homogenates were sonicated in a Bioruptor Pico (Diagenode) (15 cycles of 30 s ON/30 s OFF). After this step, the samples were centrifuged and supernatants were collected. Protein concentration was measured by Bradford assay and the samples (100 ug) were prepared for LC-MS/MS analysis using a filter-aided sample preparation (FASP) protocol (Wiśniewski *et al.*, 2009). The LC-MS/MS analysis was performed on a Q Exactive mass spectrometer (Thermo Fisher Scientific) coupled with a nanoHPLC (UltiMate 3000 RSLCnano System, Thermo Fisher Scientific), as previously described (Zacchini *et al.*, 2021). The acquired data were processed using MaxQuant software (version 1.6.7.0) (Tyanova *et al.*, 2016a) and searched with the integrated Andromeda search engine (Cox *et al.*, 2011) against the SwissProt database restricted to Mus musculus taxonomy (17 038 sequences; downloaded on 7 July 2020). The false discovery rate (FDR) for the peptide and protein identification was set to 1%. The match between runs algorithm was enabled, and label-free quantification (LFQ) was carried out. The MaxQuant output table was further processed with the use of Perseus (version 1.6.5.0) (Tyanova *et al.*, 2016b). The protein groups identified in the decoy database, contaminants and proteins only identified by site were filtered out. The LFQ intensities were log2-transformed. Student's t-test with the permutation-based FDR set to 1% was used to reveal changes between the mutant and wild-type mice. The statistical analysis was performed for the protein groups that had a minimum of 4 valid LFQ intensity values in both animal groups. The final list of differences contained proteins identified based on at least 2 peptides with a significance threshold q value of <0.01 and fold change cutoffs of 1.3 and -1.3.

All proteins selected from mass spectrometry analysis are named according to UniProt nomenclature. A PCA graph, volcano plot and hierarchical clustering were prepared with the Perseus platform (version 1.6.5.0) (Tyanova *et al.*, 2016b). Functional annotation was performed using either the Database for Annotation, Visualization and Integrated Discovery (DAVID) (Huang *et al.*, 2009a; Huang *et al.*, 2009b) tools or STRING tools (Szklarczyk *et al.*, 2023). The results were further visualised using a free online platform for data analysis and visualisation: https://www.bioinformatics.com.cn/en.

The mass spectrometry data were deposited to the ProteomeXchange Consortium (Vizcaíno *et al.*, 2014) via the MassIVE repository with the dataset identifier PXD041676.

RNA isolation and real-time PCR

Total RNA from livers was isolated using Fenozol (A&A Biotechnology), followed by spectrophotometric measurement of RNA concentration using a NanoDrop 1000 (Thermo Fisher Scientific). For reverse transcription, 1 μg of total RNA, oligo(dT) 15 primer (Promega) and M-MLV reverse transcriptase (Promega) were used. Real-time PCR was carried out using SYBR Green Master Mix (A&A Biotechnology) and a QuantStudio Real-Time PCR System (Applied Biosystems). Gene expression was normalized to *Ef2*, and then the relative transcript level was quantified by the 2^deltaCt method. The primer sequences (Sigma) are listed in Table S1 in the Supplementary Material at https://ojs.ptbioch.edu.pl/index.php/abp/.

Statistical analysis

The results are expressed as means ± SEM. One-way ANOVA with Tukey's post hoc test was applied for the comparison of multiple groups, and Student's t-test for two-group comparisons. The p-values are marked with asterisks in the charts (*p<0.05, **p<0.01 and ***p<0.001).

RESULTS

Biochemical characterisation of 'fed' and 'fasted' Mcpip1$^{fl/fl}$Alb^{Cre} mice

Deletion of Mcpip1 in liver epithelial cells leads to hepatomegaly, previously described in male mice (Kotlinowski *et al.*, 2021). As shown in Table 1, the female Mcpip1$^{fl/fl}$Alb^{Cre} animals were also characterised by larger livers and higher liver/body ratios in comparison to the Mcpip1$^{fl/fl}$ controls (Table 1). There were no differenc-

Table 1. Biochemical characteristics of Mcpip1$^{fl/fl}$ and Mcpip1$^{fl/fl}$Alb^{Cre} mice

	Fed		Fasted	
	Mcpip1$^{fl/fl}$	Mcpip1$^{fl/fl}$Alb^{Cre}	Mcpip1$^{fl/fl}$	Mcpip1$^{fl/fl}$Alb^{Cre}
Animal mass (g)	21.92±0.33	21.96±0.60	18.50±0.79###	18.23±0.39###
Liver mass (g)	0.969±0.023	1.229±0.113*	0.774±0.035p=0.09	0.985±0.018*,#
Liver/body ratio	0.045±0.001	0.056±0.004**	0.042±0.001	0.054±0.001**
Cholesterol (mmol/L)	1.70±0.14	1.77±0.16	1.70±0.10	1.68±0.10
HDL (mmol/L)	0.86±0.07	0.93±0.09	0.82±0.05	0.78±0.02
LDL (mmol/L)	0.20±0.02	0.24±0.02	0.16±0.01	0.14±0.01##
Triglycerides (mmol/L)	0.89±0.09	0.71±0.05	0.81±0.07	0.88±0.16
AST (U/L)	73.3±12.7	77.5±9.1	97.2±13.2	124.5±20.7
ALT (U/L)	30.3±6.6	35.2±5.0	21.9±3.2	31.8±6.9
Glucose (mmol/L)	6.53±0.37	6.49±0.49	3.36±0.23###	4.22±0.31*,###

Data are presented as means ± S.E.M. Data were compared using one-way ANOVA with Tukey's post hoc test, *p<0.05, **p<0.01 *vs* Mcpip1$^{fl/fl}$ and #p<0.05, ##p<0.01, ###p<0.001 *vs* counterparts from the fed group.

es in serum biochemical markers – cholesterol, HDL, LDL, triglycerides, AST, ALT and glucose – between the two groups. After 24 h of food restriction, all mice lost weight and had lower serum glucose concentrations in comparison to their fed counterparts. In the fasted group, the Mcpip1$^{fl/fl}$Alb^{Cre} animals had higher glucose concentrations than the age-matched Mcpip1$^{fl/fl}$ controls, which may suggest better adaptation to food restriction (Table 1).

Proteomic analysis revealed metabolic pathways to be affected by the lack of Mcpip1 in fasted mice

In order to investigate how Mcpip1 deletion in liver epithelial cells affects murine adaptation to fasting, we

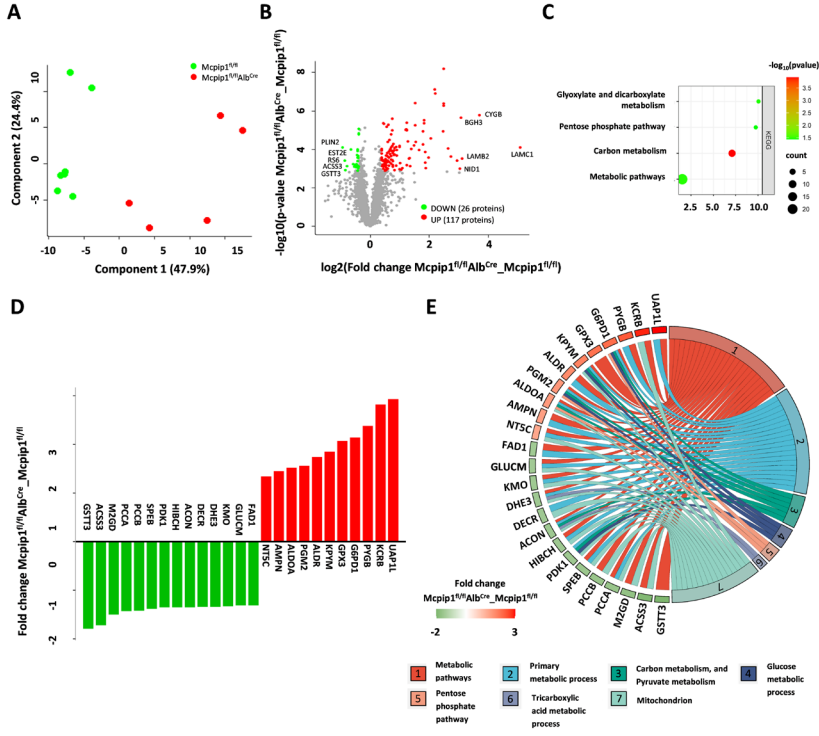

Figure 1. Metabolic pathways are affected by fasting conditions in the Mcpip1$^{fl/fl}$Alb^{Cre} animals compared to the control animals
(**A**) Substantial experimental group separation visualised by principal component analysis (PCA); (**B**) Differentially expressed proteins presented on volcano plot (shows the relationship between the fold changes (log2(FC)) and the level of significance (-log10(p-value)). Significance was marked (green – down-regulated proteins, red – up-regulated proteins) using a q-value of <0.01 and a fold change (FC) of >1.3 or <-1.3; (**C**) Bubble chart plotted by https://www.bioinformatics.com.cn/en showing enriched themes within KEGG metabolism-related pathways (results from DAVID functional annotation tool; default settings); the colour of the dots represent the significance of the enrichment; size is related to the number of changed proteins; the y-axis is the fold enrichment parameter; (**D**) Bar chart representing fold change for the differentially expressed protein related to metabolic processes (plotted by https://www.bioinformatics.com.cn/en); (**E**) Chord diagram showing the most enriched biological processes (GO terms/ KEGG pathways) with their differentially expressed proteins. green–red scale represents the fold change (plotted by https://www.bioinformatics.com.cn/en).

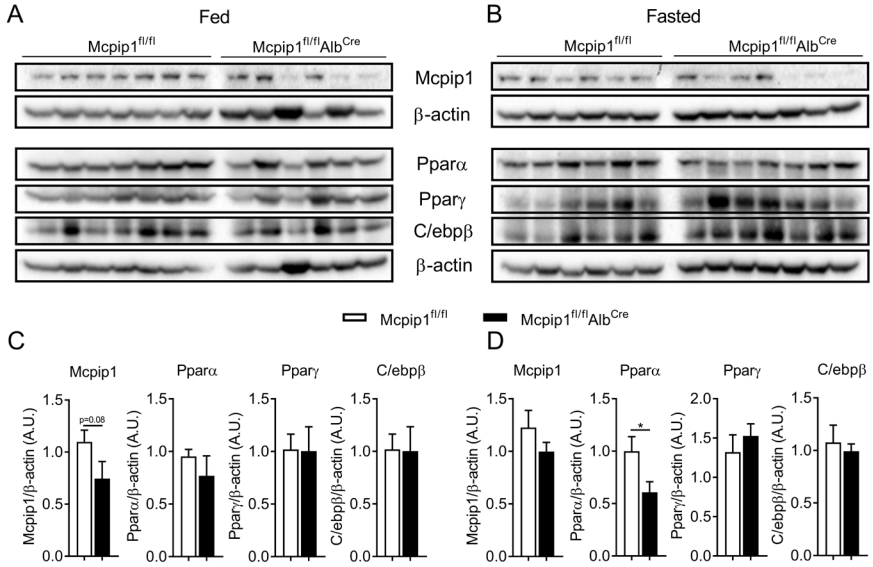

Figure 2. Levels of transcription factors regulating metabolism in livers
(**A**) Western blot analysis and **(C)** Densitometric quantification of Mcpip1, Pparα, Pparγ and C/ebpβ levels in the livers collected from Mcpip1$^{fl/fl}$ control and Mcpip1$^{fl/fl}$Alb^{Cre} knockout animals fed *ad libitum*; (**B**) Western blot analysis and (**D**) densitometric quantification of Mcpip1, Pparα, Pparγ and C/ebpβ levels in the livers collected from Mcpip1$^{fl/fl}$ control and Mcpip1$^{fl/fl}$Alb^{Cre} knockout animals after 24 h of fasting; graphs show the means + S.E.Ms; n=6–7; *p<0.05.

performed a mass spectrometry experiment utilising the label-free (LF) method. The analysis showed satisfactory separation of the groups and 143 differentially expressed proteins (Fig. 1A, Table S2 at https://ojs.ptbioch.edu.pl/index.php/abp/), 26 and 117 of which were potently down-regulated and up-regulated, respectively, in the Mcpip1$^{fl/fl}$Alb^{Cre} animals (Fig. 1B, Table S2 at https://ojs.ptbioch.edu.pl/index.php/abp/). Among the most down-regulated proteins in Mcpip1$^{fl/fl}$Alb^{Cre} mice, we identified perilipin 2 (PLIN2), pyrethroid hydrolase Ces2e (EST2E), 40S ribosomal protein S6 (RS6), acyl-CoA synthetase short-chain family member 3, mitochondrial (ACSS3) and glutathione S-transferase theta-3 (GSTT3) (Fig. 2B, green dots). Cytoglobin (CYGB), transforming growth factor-beta-induced protein ig-h3 (BGH3), laminin subunit beta-2 (LAMB2), laminin subunit gamma-1 (LAMC1) and nidogen-1 (NID1) were the most up-regulated upon Mcpip1 deletion (Fig. 2B, red dots).

In the next step, we used DAVID bioinformatics resources for functional annotation and enrichment analysis of differential proteins. We were able to distinguish several enriched biological themes among gene ontology terms and KEGG pathways (Supplementary Fig. 1A at https://ojs.ptbioch.edu.pl/index.php/abp/). A substantial number of the identified processes were related to cellular adhesion, the cytoskeleton and the extracellular matrix. Among the less affected, but still significant, we observed themes such as angiogenesis, glutathione metabolism, cell migration and proliferation. Interestingly, we also showed several processes related to the metabolic pathways that were enriched, including glyoxylate and dicarboxylate metabolism, the pentose phosphate pathway and carbon metabolism (Fig. 1C). The hierarchical clustering of proteins associated with metabolism confirmed the observed differences (Supplementary Fig. 1B at https://ojs.ptbioch.edu.pl/index.php/abp/), which were then demonstrated on the bar graph using the corresponding fold change (FC) (Fig. 1D). Fourteen and 11 proteins were significantly down-regulated and up-regulated, respectively, with an FC higher than 2 for 5 proteins: UDP-N-acetylhexosamine pyrophosphorylase-like protein 1 (UAP1L), creatine kinase B-type (KCRB), glycogen phosphorylase, brain form (PYGB), glucose-6-phosphate 1-dehydrogenase (G6PD1) and glutathione peroxidase 3 (GPX3). A more thorough analysis of those 25 proteins using the STRING software tool for known and predicted protein–protein interactions was performed and visualised on a chord diagram (Fig. 1E). As a result, we graphically demonstrated the distribution of the proteins significantly changed in our analysis within several metabolism-related themes, including the primary metabolic process, carbon and pyruvate metabolism, the glucose metabolic process, the pentose phosphate pathway, the tricarboxylic acid metabolic process and mitochondrion localisation.

Evaluation of metabolic pathways that regulate glucose and lipid turnover in the livers of Mcpip1$^{fl/fl}$ and Mcpip1$^{fl/fl}$Alb^{Cre} mice

It was already shown, that the MCPIP1 protein influences lipid metabolism by regulating C/ebpβ and Pparγ transcription factors (Lipert *et al.*, 2014). Since the turnover of lipids is a key adaptation to fasting, we also tested these proteins in the livers of control and food-restricted animals. The Mcpip1$^{fl/fl}$Alb^{Cre} mice in the fed group were characterised by lower hepatic Mcpip1 in comparison to their Mcpip1$^{fl/fl}$ counterparts, but there were no differences in the levels of Pparα, Pparγ or C/ebpβ (Fig. 2A, C). Upon fasting, hepatic Mcpip1 deletion led to a reduction of Pparα, but the other protein levels did not change (Fig. 2B, D). In the next step, we tested whether changes in protein levels resulted from different amounts of their transcripts, which might be directly regulated by Mcpip1 *via* its RNase activity. Under fed conditions, Mcpip1 deletion did not affect glycolysis (*Pkm*) – neither glycogenolysis (*Pygb*, *Pgm2*), fatty acid metabolism (*Cpt1a*, *Fabp4*, *Acox1* and *Lcad*) nor keton bodies production (*Hmgcs2*) (Fig. 3A–F). There

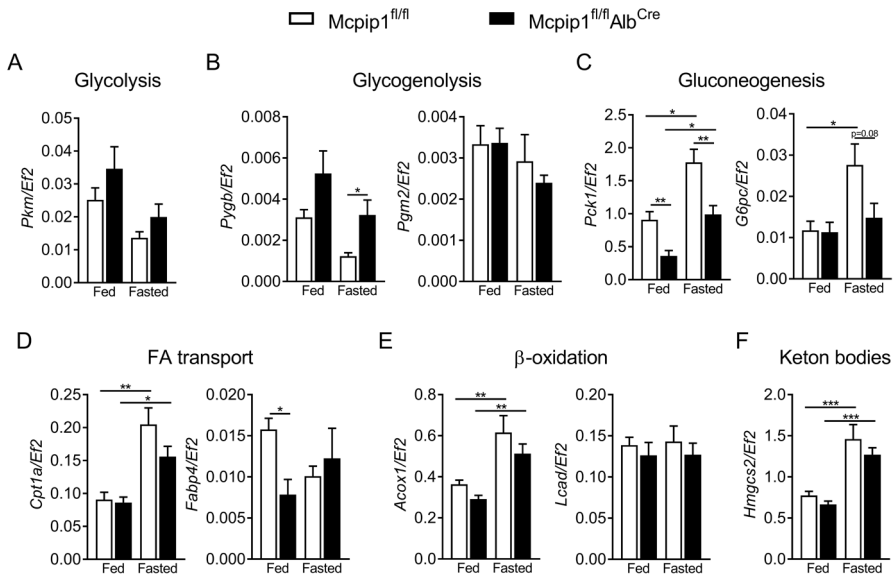

Figure 3. Hepatic Mcpip1 deletion in Mcpip1$^{fl/fl}$Alb^{Cre} mice impairs gluconeogenesis after 24 h of fasting
Expression of key enzymes regulating (**A**) glycolysis (*Pkm* – pyruvate kinase), (**B**) glycogenolysis (*Pygb* – glycogen phosphorylase; *Pgm2* – Phosphoglucomutase-2), (**C**) gluconeogenesis (*Pck1* – phosphoenolpyruvate carboxykinase 1; *G6pc* – glucose-6-phosphatase), (**D**) fatty acid transport (*Cpt1a* – carnitine palmitoyltransferase 1A; *Fabp4* – fatty acid binding protein 4), (**E**) β-oxidation (*Acox1* – peroxisomal acyl-coenzyme A oxidase 1; *Lcad* – acyl-CoA dehydrogenase, long chain) and (**F**) ketone body production (*Hmgcs2* – 3-hydroxy-3-methylglutaryl-CoA synthase 2); graphs show the means + S.E.Ms; n=6–7; *p<0.05; **p<0.01; ***p<0.001

was only a reduction in *Pck1* expression in the livers of Mcpip1$^{fl/fl}$Alb^{Cre} mice that were fed *ad libitum* (Fig. 3C). After 24 h of fasting, Mcpip1 deletion led to increased expression of *Pygb*-encoding glycogen phosphorylase, which catalyses the phosphorolysis of glycogen to yield glucose 1-phosphate (Fig. 3B). In the livers of Mcpip1$^{fl/fl}$Alb^{Cre} mice, the expression of *Pck1* and *G6pc*-encoding phosphoenolpyruvate carboxykinase 1 and glucose-6-phosphatase, respectively, was reduced in comparison to the Mcpip1$^{fl/fl}$ animals in the fasted group (Fig. 3C). Similarly to fed conditions, there were no changes in the expression of the other genes tested (Fig. 3).

DISCUSSION

The demonstration that Mcpip1$^{fl/fl}$Alb^{Cre} mice have higher serum glucose levels after food deprivation, is a major finding of this study. During fasting, hepatic glucose production relies on either glycogen breakdown or gluconeogenesis from glycerol, amino acids or TCA cycle intermediates. According to a study by Geisler *et al.*, for the first 8 hours of fasting, the serum glucose level is balanced by depletion of the hepatic glycogen content. When the duration of fasting exceeded 8 h, the researchers observed increases in hepatic gluconeogenic potential (phosphoenolpyruvate carboxykinase activity and mRNA expression) from TCA cycle intermediates (Geisler *et al.*, 2016). In line with these data, after fasting we observed increased expression of phosphoenolpyruvate carboxykinase 1 (*Pck1*) and glucose-6-phosphatase catalytic subunit (*G6pc*) – key gluconeogenic enzymes – in the livers of Mcpip1$^{fl/fl}$ mice. Although fasting did not induce *Pck1* or *G6pc* in Mcpip1$^{fl/fl}$Alb^{Cre} livers, these mice had a higher serum glucose level than their Mcpip1$^{fl/fl}$ counterparts.

According to the literature, glycogenolysis is the first adaptation to fasting and is followed by a metabolic shift toward gluconeogenesis, β-oxidation and ketogenesis – which were all observed in our experimental model. For example, the activation of β-oxidation and ketogenesis, mediated *via* induction of Cpt1 and Hmgcs2, respectively, was detected after only 12 h of food deprivation (Vilà-Brau *et al.*, 2011; Monsénégo *et al.*, 2012). In line with these results, *Hmgcs2* knockdown completely eliminates the increase in serum β-OH butyrate upon fasting (Hepler *et al.*, 2016). Although proteomic analysis did not give us a clear answer as to why Mcpip1$^{fl/fl}$Alb^{Cre} mice adapt better to fasting than Mcpip1$^{fl/fl}$ mice, we detected a few differentially expressed proteins involved in metabolic control. As shown in Fig. 1, the liver proteome of Mcpip1$^{fl/fl}$Alb^{Cre} mice significantly differed from their Mcpip1$^{fl/fl}$ counterparts when it comes to proteins involved in carbon, pyruvate and glucose metabolism, together with the pentose phosphate pathway and the tricarboxylic acid process. Perilipin 2 (PLIN2) was the most strongly down-regulated liver protein among them in the knockout animals.

Perilipin 2 belongs to a family of lipid droplet coat proteins that have emerged as physiological regulators of lipid accumulation in many tissues, including adipose and liver tissue (Ducharme & Bickel, 2008). It is constitutively located on the lipid droplet surface and has no lipolytic function, but it can block lipases, limiting triglyceride hydrolysis. Thus, the low level of perilipin 2 in Mcpip1$^{fl/fl}$Alb^{Cre} livers might facilitate triglyceride catabolism (LL *et al.*, 2007; Bell *et al.*, 2008). It was also shown that PLIN2 is the predominant lipid droplet coat protein in hepatocytes in humans and rodents subjected to NAFLD induced by a high-fat diet (Imai *et al.*, 2007). Mice with whole-body PLIN2 knockout are resistant to obesity, adipose tissue inflammation and liver steatosis when fed a high-fat diet for 12 weeks (McManaman *et al.*, 2013). Similarly, PLIN2 liver-specific ablation in mice alleviates diet-induced hepatic steatosis, inflammation, non-alcoholic steatohepatitis and liver fibrosis (Najt *et al.*, 2016; DJ *et al.*, 2019). Thus, perilipin 2 is a potentially valuable molecular target for future studies.

A growing body of evidence shows that MCPIP1 is involved in the regulation of metabolism. Its overexpression impairs adipogenesis by reducing mRNA levels of C/EBPβ and PPARγ, key transcription factors regulating this process (Lipert *et al.*, 2014). Later studies showed that MCPIP1-overexpressing adipocytes exhibit lower levels of the proteins involved in lipid and carbohydrate metabolism, and up-regulation of the proteins involved in cellular organisation and movement (Losko *et al.*, 2018). Adipocytes overexpressing MCPIP1 are additionally characterised by impaired glucose uptake due to a lower level of insulin receptor, reduced insulin-induced Akt phosphorylation and depleted Glut4 (Losko *et al.*, 2020). The level of MCPIP1 is also lower in the adipose tissue of obese subjects and in patients suffering from NAFLD (Losko *et al.*, 2018; Pydyn *et al.*, 2023). In line with these data, fatty liver disease induced by a high-fat diet in C57BL/6J mice was followed by a reduced hepatic level of Mcpip1 (Pydyn *et al.*, 2019). However, quite surprisingly, Mcpip1$^{fl/fl}$Alb^{Cre} mice on a high-fat diet for 12 weeks were not susceptible to the development of fatty liver disease. Liver fat content did not change significantly in comparison to age-matched Mcpip1$^{fl/fl}$ controls (Pydyn *et al.*, 2021).

Mcpip1 was recently described as an important regulator of hepatic homeostasis, in both physiological and pathophysiological conditions. Sun and others (Sun *et al.*, 2018) described the protective role of Mcpip1 in mice subjected to liver ischemia/reperfusion injury. Hepatocyte-specific Mcpip1 gene knockout and transgenic mice demonstrated that Mcpip1 functions to ameliorate liver damage, reduce inflammation, prevent cell death and promote regeneration. As we previously reported, the deletion of Mcpip1 in Mcpip1$^{fl/fl}$Alb^{Cre} mice led to the development of primary biliary cholangitis symptoms. In the livers of these animals, intrahepatic bile ducts displayed proliferative changes with inflammatory infiltration, bile duct destruction and fibrosis leading to cholestasis (Kotlinowski *et al.*, 2021). Massive fibrosis was already detected in young, 6-week-old Mcpip1$^{fl/fl}$Alb^{Cre} mice. Thus, the high amount of fibrosis-related or extracellular matrix proteins in the liver upon fasting was not surprising to us. Since Mcpip1 is an endoribonuclease, it is possible that some of the mRNAs encoding these proteins are direct targets of Mcpip1. In the future, it would be interesting to test whether Mcpip1 binds and digests transcripts encoding the proteins involved in the remodeling of the ECM other than MMP9 (Szukala *et al.*, 2021).

Out of 10 the most strongly up-regulated proteins, 9 were related to fibrosis. Cytoglobin (Cygb) was induced 13.1 times. In 2001 cytoglobin was discovered in hepatic stellate cells (HSCs), and it was later demonstrated to be an important regulator of HSC O_2 homeostasis under hypoxic conditions (Kawada *et al.*, 2001; Yoshizato *et al.*, 2016). Upon deletion of the *Cygb* gene in mice, hepatic O_2 homeostasis was disrupted, leading to the activation of HSCs and liver fibrosis (Yoshizato *et al.*, 2016). Cytoglobin inhibits HSC activation by maintaining its quiescent state. However, its induction in Mcpip1$^{fl/fl}$Alb^{Cre} livers does not reduce liver fibrosis in these mice, which is demonstrated by the significant overexpression of ECM-related proteins. On the contrary, in our model cytoglobin induction may result from disturbed liver homeostasis, i.e. fibrosis or inflammatory infiltration, which are both characteristic of Mcpip1$^{fl/fl}$Alb^{Cre} mice (Kotlinowski *et al.*, 2021). In fact, cytoglobin induction was already reported after long-term thioacetamide-induced liver fibrosis (Thi Thanh Hai *et al.*, 2018).

In summary, we demonstrated that hepatic deletion of Mcpip1 led to higher serum glucose concentration in mice subjected to fasting. For future studies, it would be interesting to concentrate on the liver and serum metabolome to better understand the role of Mcpip1 in metabolic homeostasis.

REFERENCES

Bell M, Wang H, Chen H, McLenithan JC, Gong D-W, Yang R-Z, Yu D, Fried SK, Quon MJ, Londos C, Sztalryd C (2008) Consequences of lipid droplet coat protein downregulation in liver cells: abnormal lipid droplet metabolism and induction of insulin resistance. *Diabetes* **57**: 2037–45. https://doi.org/10.2337/db07-1383

Cox J, Neuhauser N, Michalski A, Scheltema RA, Olsen J V, Mann M (2011) Andromeda: a peptide search engine integrated into the MaxQuant environment. *J. Proteome Res.* **10**: 1794–805. https://doi.org/10.1021/pr101065j

DJ O, AE L, ES B, RH M, J M, FG LR, JL M (2019) Perilipin-2 promotes obesity and progressive fatty liver disease in mice through mechanistically distinct hepatocyte and extra-hepatocyte actions. *J. Physiol.* **597**: https://doi.org/10.1113/JP277140

Ducharme NA, Bickel PE (2008) Lipid droplets in lipogenesis and lipolysis. *Endocrinology* **149**: 942–9. https://doi.org/10.1210/en.2007-1713

Geisler CE, Hepler C, Higgins MR, Renquist BJ (2016) Hepatic adaptations to maintain metabolic homeostasis in response to fasting and refeeding in mice. *Nutr. Metab. (Lond).* **13**: 62. https://doi.org/10.1186/s12986-016-0122-x

Goldstein I, Hager GL (2015) Transcriptional and chromatin regulation during fasting – the genomic era. *Trends Endocrinol. Metab.* **26**: 699–710. https://doi.org/10.1016/j.tem.2015.09.005

Hepler C, Foy CE, Higgins MR, Renquist BJ (2016) The hypophagic response to heat stress is not mediated by GPR109A or peripheral β-OH butyrate. *Am. J. Physiol. Regul. Integr. Comp. Physiol.* **310**: R992–R998. https://doi.org/10.1152/ajpregu.00513.2015

Hodges NJ, Innocent N, Dhanda S, Graham M (2008) Cellular protection from oxidative DNA damage by over-expression of the novel globin cytoglobin *in vitro*. *Mutagenesis* **23**: 293–298. https://doi.org/10.1093/mutage/gen013

Huang DW, Sherman BT, Lempicki RA (2009a) Systematic and integrative analysis of large gene lists using DAVID bioinformatics resources. *Nat. Protoc.* **4**: 44–57. https://doi.org/10.1038/nprot.2008.211

Huang DW, Sherman BT, Lempicki RA (2009b) Bioinformatics enrichment tools: paths toward the comprehensive functional analysis of large gene lists. *Nucleic Acids Res.* **37**: 1–13. https://doi.org/10.1093/nar/gkn923

Imai Y, Varela GM, Jackson MB, Graham MJ, Crooke RM, Ahima RS (2007) Reduction of hepatosteatosis and lipid levels by an adipose differentiation-related protein antisense oligonucleotide. *Gastroenterology* **132**: 1947–1954. https://doi.org/10.1053/j.gastro.2007.02.046

Kawada N, Kristensen DB, Asahina K, Nakatani K, Minamiyama Y, Seki S, Yoshizato K (2001) Characterization of a stellate cell activation-associated protein (STAP) with peroxidase activity found in rat hepatic stellate cells. *J. Biol. Chem.* **276**: 25318–25323. https://doi.org/10.1074/jbc.M102630200

Kotlinowski J, Hutsch T, Czyzynska-Cichon I, Wadowska M, Pydyn N, Jasztal A, Kij A, Dobosz E, Lech M, Miekus K, Pośpiech E, Fu M, Jura J, Koziel J, Chlopicki S (2021) Deletion of Mcpip1 in Mcpip1$^{fl/fl}$Alb^{Cre} mice recapitulates the phenotype of human primary biliary cholangitis. *Biochim. Biophys. Acta – Mol. Basis Dis.* **1867**: https://doi.org/10.1016/j.bbadis.2021.166086

Li M, Cao W, Liu H, Zhang W, Liu X, Cai Z, Guo J, Wang X, Hui Z, Zhang H, Wang J, Wang L (2012) MCPIP1 down-regulates IL-2 expression through an ARE-independent pathway. *PLoS One* **7**: e49841. https://doi.org/10.1371/journal.pone.0049841

Lipert B, Wegrzyn P, Sell H, Eckel J, Winiarski M, Budzynski A, Matlok M, Kotlinowski J, Ramage L, Malecki M, Wilk W, Mitus J, Jura J (2014) Monocyte chemoattractant protein-induced protein 1 impairs adipogenesis in 3T3-L1 cells. *Biochim. Biophys. Acta – Mol. Cell Res.* **1843**: 780–788. https://doi.org/10.1016/j.bbamcr.2014.01.001

Lipert B, Wilamowski M, Gorecki A, Jura J (2017) MCPIP1, alias Regnase-1 binds and cleaves mRNA of C/EBPβ. *PLoS One* **12**: e0174381. https://doi.org/10.1371/journal.pone.0174381

LL L, AG O-F, EB G, WJ B, DA B (2007) Adipocyte differentiation-related protein reduces the lipid droplet association of adipose triglyceride lipase and slows triacylglycerol turnover. *J. Lipid Res.* **48**: https://doi.org/10.1194/JLR.M700359-JLR200

Losko M, Lichawska-Cieslar A, Kulecka M, Paziewska A, Rumienczyk I, Mikula M, Jura J (2018) Ectopic overexpression of MCPIP1 impairs adipogenesis by modulating microRNAs. *Biochim. Biophys. Acta* **1865**: 186–195. https://doi.org/10.1016/j.bbamcr.2017.09.010

Losko M, Dolicka D, Pydyn N, Jankowska U, Kedracka-Krok S, Kulecka M, Paziewska A, Mikula M, Major P, Winiarski M, Budzynski A, Jura J (2020) Integrative genomics reveal a role for MCPIP1 in adipogenesis and adipocyte metabolism. *Cell. Mol. Life Sci.* **77**: 4899–4919. https://doi.org/10.1007/s00018-019-03434-5

Matsushita K, Takeuchi O, Standley DM, Kumagai Y, Kawagoe T, Miyake T, Satoh T, Kato H, Tsujimura T, Nakamura H, Akira S (2009) Zc3h12a is an RNase essential for controlling immune responses by regulating mRNA decay. *Nature* **458**: 1185–1190. https://doi.org/10.1038/nature07924

McManaman JL, Bales ES, Orlicky DJ, Jackman M, MacLean PS, Cain S, Crunk AE, Mansur A, Graham CE, Bowman TA, Greenberg AS (2013) Perilipin-2-null mice are protected against diet-induced obesity, adipose inflammation, and fatty liver disease. *J. Lipid Res.* **54**: 1346–1359. https://doi.org/10.1194/jlr.M035063

Mizgalska D, Wegrzyn P, Murzyn K, Kasza A, Koj A, Jura J, Jarzab B, Jura J (2009) Interleukin-1-inducible MCPIP protein has structural and functional properties of RNase and participates in degradation of IL-1beta mRNA. *FEBS J.* **276**: 7386–7399. https://doi.org/10.1111/j.1742-4658.2009.07452.x

Monsénégo J, Mansouri A, Akkaoui M, Lenoir V, Esnous C, Fauveau V, Tavernier V, Girard J, Prip-Buus C (2012) Enhancing liver mitochondrial fatty acid oxidation capacity in obese mice improves insulin sensitivity independently of hepatic steatosis. *J. Hepatol.* **56**: 632–639. https://doi.org/10.1016/j.jhep.2011.10.008

Moore MC, Coate KC, Winnick JJ, An Z, Cherrington AD (2012) Regulation of hepatic glucose uptake and storage in vivo. *Adv. Nutr.* **3**: 286–294. https://doi.org/10.3945/an.112.002089

Najt CP, Senthivinayagam S, Aljazi MB, Fader KA, Olenic SD, Brock JRL, Lydic TA, Jones AD, Atshaves BP (2016) Liver-specific loss of Perilipin 2 alleviates diet-induced hepatic steatosis, inflammation, and fibrosis. *Am. J. Physiol. Gastrointest. Liver Physiol.* **310**: G726–G738. https://doi.org/10.1152/ajpgi.00436.2015

Okina Y, Sato-Matsubara M, Matsubara T, Daikoku A, Longato L, Rombouts K, Thanh Thuy LT, Ichikawa H, Minamiyama Y, Kadota M, Fujii H, Enomoto M, Ikeda K, Yoshizato K, Pinzani M, Kawada N (2020) TGF-β1-driven reduction of cytoglobin leads to oxidative DNA damage in stellate cells during non-alcoholic steatohepatitis. *J. Hepatol.* **73**: 882–895. https://doi.org/10.1016/j.jhep.2020.03.051

Pydyn N, Kadluczka J, Kus E, Pospiech E, Losko M, Fu M, Jura J, Kotlinowski J (2019) RNase MCPIP1 regulates hepatic peroxisome proliferator-activated receptor gamma *via* TXNIP/PGC-1alpha pathway. *Biochim. Biophys. Acta Mol. Cell Biol. Lipids* **1864**: 1458–1471. https://doi.org/10.1016/j.bbalip.2019.06.006

Pydyn N, Żurawek D, Koziel J, Kus E, Wojnar-Lason K, Jasztal A, Fu M, Jura J, Kotlinowski J (2021) Role of Mcpip1 in obesity-induced hepatic steatosis as determined by myeloid and liver-specific conditional knockouts. *FEBS J.* **288**: 6563–6580. https://doi.org/10.1111/febs.16040

Pydyn N, Kadluczka J, Major P, Hutsch T, Belamri K, Malczak P, Radkowiak D, Budzynski A, Miekus K, Jura J, Kotlinowski J (2023) Hepatic MCPIP1 protein levels are reduced in NAFLD patients and are predominantly expressed in cholangiocytes and liver endothelium. *Hepatol. Commun.* **7**: e0008. https://doi.org/10.1097/HC9.0000000000000008

Sun P, Lu Y-X, Cheng D, Zhang K, Zheng J, Liu Y, Wang X, Yuan Y-F, Tang Y-D (2018) Monocyte chemoattractant protein-induced protein 1 targets hypoxia-inducible factor 1α to protect against hepatic ischemia/reperfusion injury. *Hepatology* **68**: 2359–2375. https://doi.org/10.1002/hep.30086

Szklarczyk D, Kirsch R, Koutrouli M, Nastou K, Mehryary F, Hachilif R, Gable AL, Fang T, Doncheva NT, Pyysalo S, Bork P, Jensen LJ, von Mering C (2023) The STRING database in 2023: protein-protein association networks and functional enrichment analyses for any sequenced genome of interest. *Nucleic Acids Res.* **51**: D638–D646. https://doi.org/10.1093/nar/gkac1000

Szukala W, Lichawska-Cieslar A, Pietrzycka R, Kulecka M, Rumienczyk I, Mikula M, Chlebicka I, Konieczny P, Dziedzic K, Szepietowski JC, Fontemaggi G, Rys J, Jura J (2021) Loss of epidermal MCPIP1 is associated with aggressive squamous cell carcinoma. *J. Exp. Clin. Cancer Res.* **40**: 391. https://doi.org/10.1186/s13046-021-02202-3

Thi Thanh Hai N, Thuy LTT, Shiota A, Kadono C, Daikoku A, Hoang DV, Dat NQ, Sato-Matsubara M, Yoshizato K, Kawada N (2018) Selective overexpression of cytoglobin in stellate cells attenuates thioacetamide-induced liver fibrosis in mice. *Sci. Rep.* **8**: 17860. https://doi.org/10.1038/s41598-018-36215-4

Tyanova S, Temu T, Cox J (2016a) The MaxQuant computational platform for mass spectrometry-based shotgun proteomics. *Nat. Protoc.* **11**: 2301–2319. https://doi.org/10.1038/nprot.2016.136

Tyanova S, Temu T, Sinitcyn P, Carlson A, Hein MY, Geiger T, Mann M, Cox J (2016b) The Perseus computational platform for comprehensive analysis of (prote)omics data. *Nat. Methods* **13**: 731–40. https://doi.org/10.1038/nmeth.3901

Vilà-Brau A, De Sousa-Coelho AL, Mayordomo C, Haro D, Marrero PF (2011) Human HMGCS2 regulates mitochondrial fatty acid oxidation and FGF21 expression in HepG2 cell line. *J. Biol. Chem.* **286**: 20423–30. https://doi.org/10.1074/jbc.M111.235044

Vizcaíno JA, Deutsch EW, Wang R, Csordas A, Reisinger F, Ríos D, Dianes JA, Sun Z, Farrah T, Bandeira N, Binz PA, Xenarios I, Eisenacher M, Mayer G, Gatto L, Campos A, Chalkley RJ, Kraus HJ, Albar JP, Martinez-Bartolomé S, Apweiler R, Omenn GS, Martens L, Jones AR, Hermjakob H (2014) ProteomeXchange provides globally coordinated proteomics data submission and dissemination. *Nat. Biotechnol.* **32**: 223–6. https://doi.org/10.1038/nbt.2839

Wiśniewski JR, Zougman A, Nagaraj N, Mann M (2009) Universal sample preparation method for proteome analysis. *Nat. Methods* **6**: 359–62. https://doi.org/10.1038/nmeth.1322

Yoshizato K, Thuy LTT, Shiota G, Kawada N (2016) Discovery of cytoglobin and its roles in physiology and pathology of hepatic stellate cells. *Proc. Jpn. Acad. Ser. B Phys. Biol. Sci.* **92**: 77–97. https://doi.org/10.2183/pjab.92.77

Zacchini F, Heber MF, Arena R, Radczuk N, Jankowska U, Ptak GE (2021) Perturbations of the hepatic proteome behind the onset of metabolic disorders in mouse offspring developed following embryo manipulation. *Theriogenology* **171**: 119–129. https://doi.org/10.1016/j.theriogenology.2021.05.022